

# NMR Study of Strontium Binding by a Micaceous Mineral

Geoffrey M. Bowers,<sup>†</sup> Ramesh Ravella,<sup>‡</sup> Sridhar Komarneni,<sup>‡</sup> and Karl T. Mueller<sup>\*,†</sup>

Department of Chemistry and Department of Crop and Soil Sciences, Penn State University,  
University Park, Pennsylvania, 16802

Received: December 9, 2005; In Final Form: February 16, 2006

The nature of strontium binding by soil minerals directly affects the transport and sequestration/remediation of radioactive strontium species released from leaking high-level nuclear waste storage tanks. However, the molecular-level structure of strontium binding sites has seldom been explored in phyllosilicate minerals by direct spectroscopic means and is not well-understood. In this work, we use solid-state NMR to analyze strontium directly and indirectly in a fully strontium-exchanged synthetic mica of nominal composition  $\text{Na}_4\text{Mg}_6\text{Al}_4\text{Si}_4\text{O}_{20}\text{F}_4$ . Thermogravimetric analysis, X-ray diffraction analysis, and NMR evidence supports that heat treatment at 500 °C for 4 h fully dehydrates the mica, creating a hydrogen-free interlayer. Analysis of the strontium NMR spectrum of the heat-treated mica shows a single strontium environment with a quadrupolar coupling constant of 9.02 MHz and a quadrupolar asymmetry parameter of 1.0. These quadrupolar parameters are consistent with a highly distorted and asymmetric coordination environment that would be produced by strontium cations without water in the coordination sphere bound deep within the ditrigonal holes. Evidence for at least one additional strontium environment, where proton–strontium couplings may occur, was found via a  $^1\text{H}$ – $^{87}\text{Sr}$  transfer of populations by double resonance NMR experiment. We conclude that the strontium cations in the proton-free interlayer are observable by  $^{87}\text{Sr}$  NMR and bound through electrostatic interactions as nine coordinate inner-sphere complexes sitting in the ditrigonal holes. Partially hydrated strontium cations invisible to direct  $^{87}\text{Sr}$  NMR are also present and located on the external mica surfaces, which are known to hydrate upon exposure to atmospheric moisture. These results demonstrate that modern pulsed NMR techniques and high fields can be used effectively to provide structural details of strontium binding by phyllosilicate minerals.

## Introduction

Strontium-90 is a radionuclide with a half-life of 29.1 years and the second most abundant radioactive contaminant released from the 1986 Chernobyl accident.<sup>1</sup> It is also the second most abundant radionuclide found in high-level liquid nuclear waste resulting from plutonium isolation and purification processes.<sup>2</sup> At sites such as Hanford and other former U.S. Department of Energy (DOE) plutonium production facilities, caustic nuclear waste (and, therefore,  $^{90}\text{Sr}$ ) has leaked from underground waste storage tanks into the soil<sup>3,4</sup> and is believed to cause subsequent mineral transformation reactions that form zeolite-like precipitated phases.<sup>5</sup> As organisms readily incorporate ~15% of any metabolized strontium into bone mass,<sup>6–8</sup>  $^{90}\text{Sr}$  is arguably the most biologically hazardous component of the high-level waste, and, therefore, the subsequent transport and remediation of  $^{90}\text{Sr}$  released from the waste storage tanks represent issues of great importance to the DOE and the general public.

Recently, Komarneni and co-workers have developed a strontium- and radium-selective mica that sequesters these cations at environmentally relevant pHs.<sup>9–11</sup> The mica has a nominal composition of  $\text{Na}_4\text{Mg}_6\text{Al}_4\text{Si}_4\text{O}_{20}\text{F}_4$  (Na-4 mica) and contains three unique features as synthesized: (i) there are no structural protons in the mica, (ii) the charge-balancing cation is sodium rather than potassium, and (iii) the successive layers

are offset from each other by roughly one-third of the unit cell's  $b$  dimension. A monolayer of water is readily sorbed into the interlayer when sodium is the charge-balancing cation, expanding the interlayer spacing from 0.4 to 2.8 Å. In the latter state, strontium or radium can enter the interlayer and exchange with the sodium cations. In a recent report focusing on radium binding,<sup>12</sup> strong electrostatic interactions between the radium and the interlayer surfaces were shown to force water out of the interlayer, collapsing it to 0.6 Å. Komarneni has hypothesized that this collapse is also accompanied by a shift of the adjacent layers, removing the offset and producing a 12-coordinate radium cation spanning the gap between adjacent layers.<sup>12</sup> To test this hypothesis and determine whether it applies to strontium binding as well, we must employ spectroscopic techniques capable of providing a detailed, atomic-level understanding of strontium and radium sorption.

To date, only extended X-ray absorption fine structure (EXAFS) and related X-ray techniques have been used to investigate the coordination environment of strontium nuclei in layered minerals. Chen et al. performed EXAFS and other X-ray absorption spectroscopy studies of strontium bound by kaolinite, illite, hectorite, and montmorillonite, while varying the pH and ionic strength of the electrolyte-exchange solution.<sup>13–15</sup> In all cases, they conclude that strontium–oxygen distances in the first shell are consistent with strontium sorption as a six-coordinate outer-sphere complex in hydrated forms of these minerals. Sahai et al. examined three systems with EXAFS, where the only available cation sorption sites are on external surfaces (kaolinite, goethite, and amorphous silica) and also

\* Corresponding author. E-mail: ktm2@psu.edu. Phone: 814-863-8674. Fax: 814-863-8403.

<sup>†</sup> Department of Chemistry.

<sup>‡</sup> Department of Crop and Soil Sciences.

concluded that strontium sorption in these cases occurs via outer-sphere complexation.<sup>16</sup> However, their EXAFS data suggest that these strontium nuclei are coordinated by nine water molecules.<sup>16</sup> O'Day et al. used EXAFS to examine strontium sorbed by the natural zeolite heulandite and determined that strontium is sequestered as a partially hydrated inner-sphere complex at the Ca2 site of the zeolite's *B* channel.<sup>17</sup> None of the available EXAFS literature includes studies of fully *dehydrated* minerals with both interlayer and surface sorption sites available to strontium.

An alternative and often complementary tool to EXAFS for molecular-level structure determination is solid-state NMR spectroscopy. NMR provides one primary advantage over X-ray techniques for these analyses, namely, an ability to distinguish among unique cation environments in a model-free manner, especially in cases where each site produces a unique set of spectral features. Solid-state NMR is, therefore, ideally suited for studies of strontium binding in minerals with multiple unique sorption environments. For quadrupolar nuclei like  $^{87}\text{Sr}$  (the only stable NMR-active isotope of strontium), NMR parameters such as the quadrupolar coupling constant ( $C_q$ ) and quadrupolar asymmetry parameter ( $\eta$ ) are highly sensitive to changes in the local electronic environment. These parameters, therefore, provide a means to directly probe the binding mechanism and binding structure(s) of strontium sorbed by (alumino)silicate minerals in both model and real (heterogeneous) systems. In addition, double-resonance methods, such as the transfer of populations by double resonance (TRAPDOR) technique,<sup>18–20</sup> provide a means to exploit through-space interactions between nuclei and detect strontium indirectly via interactions with other, more abundant, spins.

Solid-state NMR studies of  $^{87}\text{Sr}$  have been rather scarce in the literature<sup>21–26</sup> to date as NMR signals from this low gyromagnetic ratio nucleus suffer from severe sensitivity limitations (the receptivity compared to  $^1\text{H}$  is  $5.7 \times 10^{-6}$ ). Opportunely, recent advances have improved our ability to directly probe low-gamma quadrupolar nuclei such as  $^{87}\text{Sr}$  in powdered samples. The quadrupolar Carr–Purcell–Meiboom–Gill (QCPMG) sequence<sup>27,28</sup> and the double-frequency sweep (DFS) preparatory scheme<sup>29</sup> have each been shown to provide up to 10-fold enhancement to the signal-to-noise ratio when applied to other nuclei.<sup>22,29–35</sup> The properties of  $^{87}\text{Sr}$  also make this nucleus an ideal candidate for study using modern ultrahigh field spectrometers, where the increased field strength provides enhancements due to the Curie law, narrowing of the spectral resonances, and the associated increase in the strontium resonance frequency.<sup>23,36</sup> However, despite these benefits and the successful implementation of high-field  $^{87}\text{Sr}$  QCPMG experiments in studies of inorganic salts,<sup>22,23</sup> the direct observation of strontium nuclei in complex minerals has remained elusive to date.

In this work, we apply  $^{87}\text{Sr}$  DFS-QCPMG at 21.14 T and  $^1\text{H}$ – $^{87}\text{Sr}$  TRAPDOR NMR at 11.74 T to analyze strontium binding in strontium-saturated and heat-treated Na-4 mica. We demonstrate that DFS-QCPMG NMR at 21.14 T provides sufficient sensitivity for direct observation of strontium bound in the mica interlayer following heat treatment at 500 °C. We also show that  $^1\text{H}$ – $^{87}\text{Sr}$  TRAPDOR NMR can be used to detect externally bound strontium cations that are difficult or impossible to observe by direct  $^{87}\text{Sr}$  NMR. We use the results of the NMR analyses to deduce the nature of strontium binding by the heat-treated mica and propose a binding structure for strontium in the interlayer.

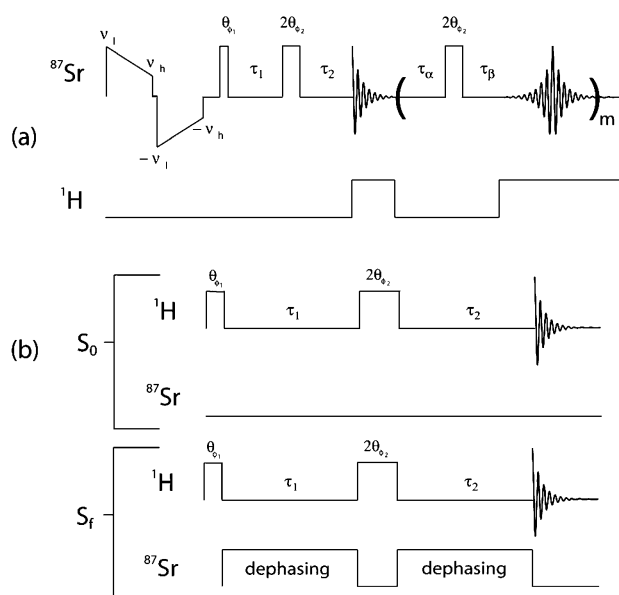


**Figure 1.** Schematic representations of (a) the  $^1\text{H}$ -decoupled DFS-QCPMG sequence and (b) both components of the TRAPDOR sequence.

## Experimental Section

**Mica Preparation and X-ray Diffraction (XRD).** The mica was prepared according to a modified procedure of Komarneni et al.<sup>9</sup> and Paulus et al.<sup>37</sup> This synthesis procedure is designed specifically to exclude hydrogen atoms from the mica structure; each Mg–OH species one would expect to find in the octahedral sheet of a trioctahedral mica is replaced in this material with an Mg–F moiety. Following the synthesis, the Na-4 mica was saturated with  $\text{Sr}^{2+}$  ions. Full saturation with strontium yields a theoretical loading of roughly 468 mequiv of strontium per 100 g of mica. Thermogravimetric analysis (TGA) was performed on the saturated mica to help design a heat-treatment procedure that will completely dehydrate the mica, providing a proton-free interlayer. Based on the TGA results, a portion of the mica was heated at 500 °C for 4 h to drive off interlayer and surface-sorbed water. XRD analyses were performed to monitor the *d* spacing before and after heat treatment using a Scintag diffractometer operated at 35 kV with a 30 mA current and Cu–K $\alpha$  radiation ( $\lambda = 1.54178 \text{ \AA}$ ).

**$^{87}\text{Sr}$  NMR.** The NMR experiments used to directly probe the  $^{87}\text{Sr}$  nuclei incorporated a DFS preparatory scheme<sup>29</sup> combined with the QCPMG pulse sequence<sup>27,28</sup> and  $^1\text{H}$  decoupling at a magnetic field strength of 21.14 T (Figure 1a). The 5-mm cross-coil static probe<sup>38</sup> and 21.14 T Varian Inova spectrometer used in this study are available in the high-field magnetic resonance user facility at the Pacific Northwest National Laboratory. At the beginning of each acquisition cycle, frequency regions of 1.5 MHz ( $\nu_l$ ) to 50 kHz ( $\nu_h$ ) from the transmitter frequency were swept over 1 ms at a central transition  $\nu_{rf}$  of 65 kHz. This set of sweep conditions was found to maximize the sensitivity enhancement provided by DFS preparation (in this case, approximately a factor of 4 in signal-to-noise ratio). A data sampling rate of 1 MHz was used in conjunction with a receiver bandwidth of 200 kHz to allow for rapid digitization, with the filter bandwidth restricted to a region near the edges of the excitation profile. A selective  $\theta = \pi/2$  pulse width of  $3.8 \mu\text{s}$  was used in combination with  $\tau$  delays of  $\tau_1 = \tau_\alpha = 100 \mu\text{s}$  and  $\tau_2 = \tau_\beta = 110.5 \mu\text{s}$ . The evolution periods after each pulse are longer than those before the pulses to account for the delay associated with the particular filter

window; the additional delay of 10.5  $\mu$ s was found empirically to ensure the first data point in the NMR signal corresponds to an echo maximum. After the initial  $\pi/2 - \pi$  echo sequence and half-echo acquisition, forty refocusing pulses were applied, where each pulse is followed by the acquisition of a full echo. A spikelet spacing of 1 kHz was produced by acquiring 500 data points per half echo, resulting in a total acquisition length of 40 500 points that was then zero-filled until the total data set contained 262 144 points before Fourier transformation. Proton decoupling was applied during data acquisition using a continuous wave pulse at a power level of 200 W. A total of 150 000 transients were collected over a period of 67 h to produce the final strontium spectra. The “comb filter” apodization scheme originally proposed by Lipton and co-workers<sup>32</sup> was applied to the signal before transformation to the frequency domain. In this case, 4 kHz of exponential apodization was applied to each individual echo rise and decay, maintaining the signal intensity of each echo maximum while reducing the noise level between maxima. The mica spectra were referenced to a 1 M aqueous solution of  $\text{SrCl}_2$  prepared from  $\text{SrCl}_2 \cdot 6\text{H}_2\text{O}$  (obtained from Sigma-Aldrich). Iterative simulations of the spectra were performed using real pulse conditions and 8000 repulsion-based crystallite orientations using the SIMPSON program by Bak and co-workers.<sup>39</sup> The full simulation required 6 h to complete on the Lion-XO computing cluster at the Pennsylvania State University using 32 2.4-GHz AMD Opteron processors with 8 GB of RAM allocated to each processor.

**$^1\text{H}$ – $^{87}\text{Sr}$  TRAPDOR.** TRAPDOR NMR experiments<sup>18,19</sup> with proton detection and strontium dephasing were performed on an 11.74 T Varian Infinity spectrometer using the  $^1\text{H}$  and low-frequency channels of a 5-mm triple resonance magic angle spinning (MAS) probe with the sample spinning at 10 kHz. In this experiment,  $^1\text{H}$  nuclei that are strongly coupled to strontium nuclei through the direct dipolar interaction (which has an inverse  $r^{-3}$  dependence on the internuclear distance  $r$ ) can be identified. The TRAPDOR experiment is a “difference” experiment, where two signals are acquired:  $S_0$  without hydrogen/strontium dipolar dephasing and  $S_f$  with dipolar dephasing. The subtraction of  $S_f$  from  $S_0$  isolates the resonances of hydrogen species closely associated with the strontium nuclei. A  $^1\text{H}$   $\pi/2$  pulse width of 10  $\mu$ s was used with a sweep width of 100 kHz to acquire both the  $S_0$  and the  $S_f$  signals (Figure 1b). One thousand transients were acquired with a 5 s pulse delay over a 90 min period for both  $S_0$  and  $S_f$ . Exponential apodization corresponding to 300 Hz of line-broadening was applied to the time-domain signals before transformation to the frequency domain and calculation of the TRAPDOR difference spectrum. Because TRAPDOR is a difference experiment, the proton background of the system is automatically canceled during the processing of the TRAPDOR data and, thus, is not an issue. Chemical shifts are referenced to tetramethylsilane through a secondary standard from the residual  $^1\text{H}$  species in  $\text{D}_2\text{O}$  at 298 K.

## Results and Discussion

**Effects of the Heat Treatment.** In all of our  $^{87}\text{Sr}$  studies, we have yet to observe a  $^{87}\text{Sr}$  NMR resonance in any inorganic salt, phyllosilicate mineral, or tectosilicate mineral when strontium includes water in the coordination sphere, providing strong evidence that strontium nuclei with any degree of hydration may not be observable directly by  $^{87}\text{Sr}$  NMR (a matter currently under investigation in our laboratory). By heating the mica to drive off interlayer moisture, anhydrous strontium cations will be present in the mica interlayer that should be

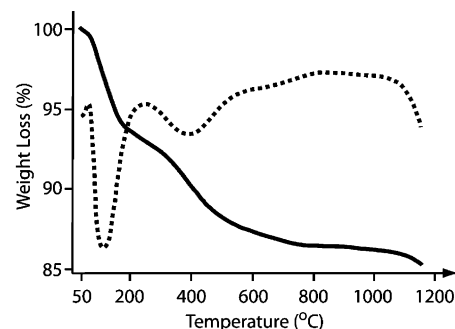


**Figure 2.** TGA (solid) and derivative TGA (dashed) curves from Na-4 mica. Both minima below 500  $^{\circ}\text{C}$  in the derivative curve represent the loss of water.

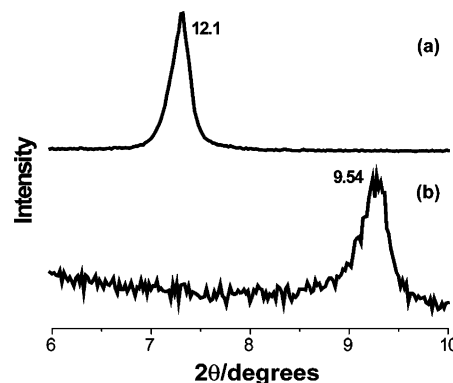


**Figure 3.** XRD pattern of (a) the unheated mica saturated with strontium and (b) the strontium-saturated and heat-treated mica.

observable by  $^{87}\text{Sr}$  NMR. Therefore, the aim of the heat treatment was to fully dehydrate the mica prior to performing the NMR experiments. As stated in the Experimental Section, TGA analyses were performed to determine a temperature program capable of removing all interlayer water from the Na-4 mica. The TGA curve shows an initial weight loss of approximately 7% that occurs below a temperature of approximately 120  $^{\circ}\text{C}$  (Figure 2), associated with the removal of loosely bound water molecules. A similar weight loss has been reported in the literature for a pure Na-4 mica phase and was attributed to the removal of  $3.6 \pm 0.3$  water molecules per unit cell; a nearly stoichiometric amount of interlayer water.<sup>40</sup> A second broad peak occurs in the derivative curve with a minimum near 400  $^{\circ}\text{C}$ , corresponding to the loss of residual tightly sorbed water. No additional losses occur through 1200  $^{\circ}\text{C}$ , indicating that full removal of water is achieved before a temperature of approximately 450  $^{\circ}\text{C}$ . A 4 h heat treatment at 500  $^{\circ}\text{C}$  is, therefore, appropriate to remove all interlayer and surface-sorbed water from the mica.

To confirm the effectiveness of the proposed heat treatment, XRD analyses were performed on mica samples before and after heating to monitor the  $d$  spacing, which should collapse to 9.4–9.8  $\text{\AA}$  with the loss of all interlayer water. Indeed, the Sr-saturated mica showed a  $d$  spacing of 12.1  $\text{\AA}$  that collapsed to approximately 9.6  $\text{\AA}$  (a change in interlayer spacing from 2.7 to 0.2  $\text{\AA}$ ) upon heating, consistent with the removal of all interlayer water molecules (Figure 3). Proton-decoupled DFS-QCPMG  $^{87}\text{Sr}$  NMR experiments also confirm the absence of interlayer water. Figure 4 contains proton-decoupled DFS-QCPMG  $^{87}\text{Sr}$  NMR spectra acquired under identical experimental conditions of strontium-saturated Na-4 mica with and without heat treatment. Note that there is no detectable  $^{87}\text{Sr}$  signal from the hydrated sample, consistent with our findings in other systems where water is coordinated to strontium cations,

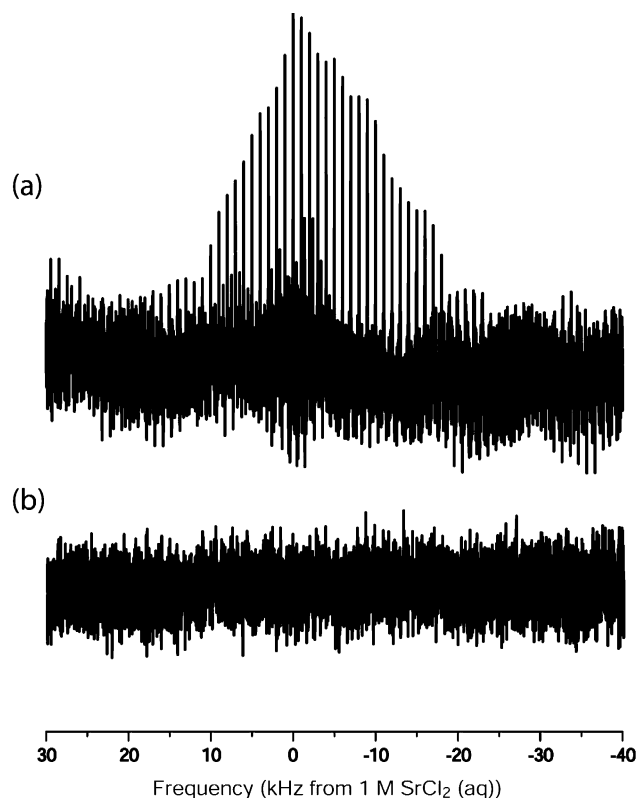


**Figure 4.** Proton-decoupled  $^{87}\text{Sr}$  DFS-QCPMG NMR spectra of dehydrated (a) and hydrated (b) Na-4 mica. Note that no observable signal appears in the spectrum of the hydrated mica.

but a strontium signal is observed in the heated mica. This suggests that  $^{87}\text{Sr}$  DFS-QCPMG NMR will be selective for anhydrous interlayer strontium in the heated Na-4 mica and that strontium bound to the mica exterior (the surface of which will spontaneously hydrate upon exposure to atmospheric moisture) may only be observable with indirect double resonance techniques, such as  $^1\text{H}$ – $^{87}\text{Sr}$  TRAPDOR NMR.

**$^{87}\text{Sr}$  NMR Spectra and Interlayer Strontium Binding.** As indicated in Figure 4, a single strontium resonance was observed from the heated mica sample after a 67 h acquisition period using  $^1\text{H}$ -decoupled DFS-QCPMG at 21.14 T. This represents a marked sensitivity enhancement compared to that of commonly utilized NMR techniques; our best estimations show that performing the same analysis at a more conventional field strength (11.74 T) would require approximately 1800 days (roughly 4.9 years) to complete. Strontium cations bound to the external mica surface cannot be responsible for the observed  $^{87}\text{Sr}$  NMR signal, because the external mica surface is known to hydrate upon exposure to the atmosphere, leading to at least partially hydrated strontium cations invisible to direct  $^{87}\text{Sr}$  NMR. We conclude that the  $^{87}\text{Sr}$  resonance is associated with the strontium cations bound in the proton-free interlayer.

Insight into the nature of the interlayer strontium binding environment can also be drawn from the  $^{87}\text{Sr}$  NMR spectrum. If the twelve-coordinate binding model proposed for radium holds for strontium, the strontium cation will be located at the center of a symmetric coordination environment where quadrupolar effects would be negligible, leading to a narrow  $^{87}\text{Sr}$  line shape. However, the strontium resonance observed in the heat-treated mica has significant quadrupolar character and is well-fit by a single quadrupolar line shape, with a coupling constant of 9.02 MHz and an asymmetry parameter of 1.0 (Figure 5).<sup>39</sup> Furthermore, if the strontium cations span the interlayer space, as in the dehydrated radium model, we would

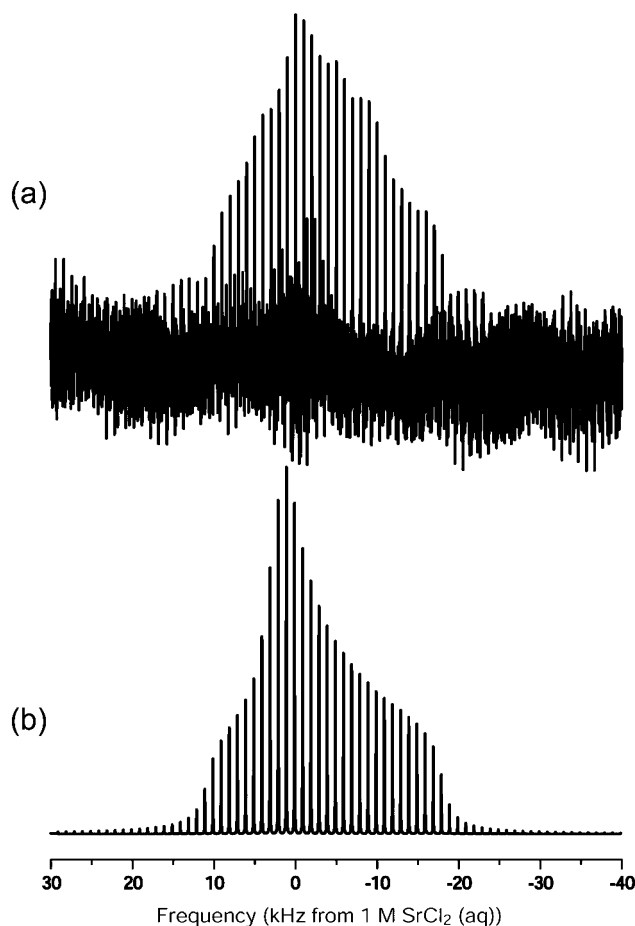


**Figure 5.** Experimental (a) and simulated (b)  $^{87}\text{Sr}$  QCPMG NMR spectra from the heated mica.

expect to observe an interlayer spacing of roughly 0.4 Å rather than the 0.2 Å that is observed with XRD. Thus, the binding mechanism of the interlayer strontium cannot be the same as the twelve-coordinate interlayer radium-binding model.<sup>12</sup>

Quadrupolar parameters of this magnitude (especially the asymmetry parameter) have been associated only with highly distorted strontium coordination environments,<sup>23</sup> suggesting that the strontium cations contributing to the resonance possess an asymmetric coordination sphere. Within the anhydrous interlayer, such an asymmetry can be envisioned for strontium cations bound through electrostatic interactions within the ditrigonal holes (where a large electron density is available). In this situation, strontium cations would not span the interlayer space, and the driving force of strong electrostatic interactions required to induce a layer shift will be absent. To facilitate full charge compensation in a nonshifted case, we expect the interlayer strontium cations to include the two nearest oxygen atoms on the opposite interlayer surface in the coordination sphere, producing an electrostatically driven nine-coordinate asymmetric strontium binding site (Figure 6). This coordination environment is also consistent with the 0.2 Å interlayer spacing observed with XRD. Furthermore, basic steric considerations argue that strontium cations are more likely to bind within the ditrigonal holes than radium cations because the strontium ionic radius is roughly 0.2 Å smaller than that of radium.

The nine-coordinate interlayer binding model proposed here incorporates the fluorine from the Mg–F species into the strontium coordination sphere. The high electronegativity of fluorine contributes to the rich electron density present in the ditrigonal holes, helping to draw the strontium cations down



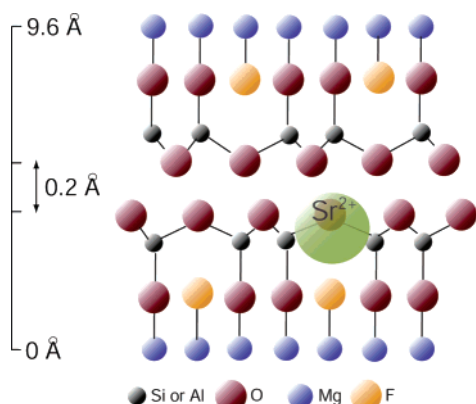


**Figure 6.** Cross-sectional representation (not to scale) of the mica structure with interlayer strontium sitting in the ditrigonal hole of the tetrahedral sheet. The strontium is partially transparent in the figure to permit visualization of its position within the hole.

out of the interlayer. However, bringing the strontium nucleus close in space to the fluorine creates the potential for strontium–fluorine couplings that may affect the  $^{87}\text{Sr}$  NMR spectrum. To determine the extent of such effects, we calculated the two spin  $^{19}\text{F}$ – $^{87}\text{Sr}$  dipolar coupling as a function of internuclear distance. The magnitude of this interaction was found to be only 613 Hz at the shortest possible internuclear distance of 2.04 Å (fluorine atomic radius = 0.72 Å and strontium ionic radius = 1.32 Å). This coupling strength is significantly less than the  $\approx 9$  MHz quadrupolar coupling that leads to a static line width of approximately 30 kHz. A dipolar coupling of this magnitude should, therefore, have little effect on the strontium spectrum. To confirm this assertion, SIMPSON simulations of the strontium resonance incorporating this maximal dipolar coupling were performed. The simulation results did not show a significant effect in the shape of the  $^{87}\text{Sr}$  NMR spectrum, permitting us to conclude that the presence of fluorine in the strontium coordination sphere does not significantly influence the resonance line shape or width.

#### $^1\text{H}$ – $^{87}\text{Sr}$ TRAPDOR and Externally Bound Strontium.

The findings presented in the available EXAFS literature, specifically the observation of strontium sorption to external mineral surfaces via outer-sphere complexation, suggests that strontium sorbed to the external surface of the heated mica will spontaneously hydrate upon exposure to the ambient atmosphere.<sup>14,16</sup> In an attempt to detect the presence of at least partially hydrated surface-strontium species in the heated mica, a  $^1\text{H}$ – $^{87}\text{Sr}$  TRAPDOR experiment was performed to identify hydrogen species closely associated with strontium. Two well-resolved peaks appear in the TRAPDOR difference spectrum (Figure 7): one at a chemical shift of 3.6 ppm and the other at roughly 0 ppm. The peak at 3.6 ppm is tentatively assigned to the protons on water molecules sorbed to the external silica surfaces of mica particles; it is well-documented in the solid-state NMR literature that proton peaks shift upfield with increasingly strong hydrogen-bonding interactions, and proton shifts of  $\sim 3.5$  ppm have been assigned to waters sorbed by silica surfaces.<sup>41</sup> The origin of the second peak is not as clear and cannot be discussed in detail. Some potential sources of this second resonance include (i) waters of hydration on the strontium nucleus that are not interacting with the external silica surfaces of the mica, (ii) interactions of silanol groups on the mica surfaces with strontium cations, or (iii) minor impurity phases containing hydrated strontium cations. Because TRAPDOR is not inherently quantitative and there are a number of potential sources of  $^1\text{H}$ – $^{87}\text{Sr}$  interactions, the number of unique

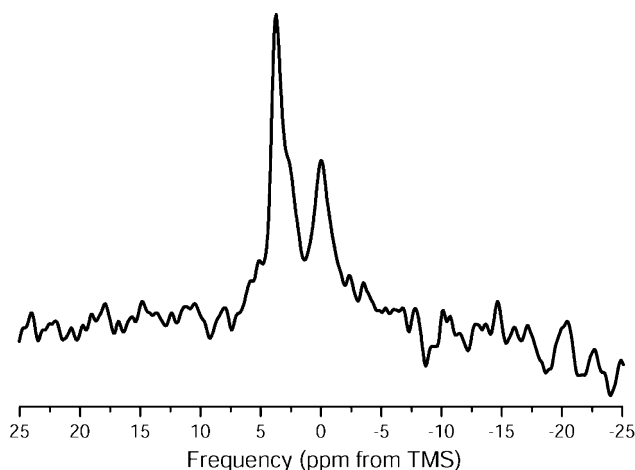


**Figure 7.**  $^1\text{H}$ – $^{87}\text{Sr}$  TRAPDOR difference spectrum.

external strontium environments cannot be deduced from the TRAPDOR data alone and will not be speculated upon further in this paper. However, the TRAPDOR results do support the existence of surface-sorbed and partially hydrated strontium, as predicted from the EXAFS literature.

Despite our successful observation of surface and interlayer strontium species in the heated, strontium-saturated mica, studies of phyllosilicates with environmentally relevant levels of strontium remain elusive. The additional sensitivity enhancement gained from DFS preparation is insufficient to enable strontium detection by solid-state NMR with significantly fewer  $^{87}\text{Sr}$  spins. Other methods of sensitivity enhancement may provide the necessary gains in signal-to-noise ratio to enable  $^{87}\text{Sr}$  NMR studies of low-strontium content materials. Decreasing the temperature to enhance the population difference across the  $^{87}\text{Sr}$  central transition is one potential solution, as low-temperature methods have been used to identify individual  $^{67}\text{Zn}$  and  $^{25}\text{Mg}$  cations bound by metalloproteins.<sup>32</sup> Rotor-synchronized MAS-QCPMG NMR is another alternative given that MAS will decrease the width of the quadrupolar pattern and provide additional enhancement. The applicability of these techniques to  $^{87}\text{Sr}$  NMR is currently being explored.

#### Conclusion

In this paper, the interlayer and putative surface-bound strontium in a dehydrated phyllosilicate mineral have been analyzed with solid-state NMR. We have presented NMR, TGA, and XRD evidence that the anhydrous interlayer strontium is bound through electrostatic interactions as a nine-coordinate species residing in the ditrigonal holes of the tetrahedral sheets. We also demonstrated that  $^1\text{H}$ – $^{87}\text{Sr}$  TRAPDOR NMR can detect surface-sorbed strontium cations apparently invisible to  $^{87}\text{Sr}$  DFS-QCPMG NMR through their interactions with proton-bearing surface species. This study demonstrates that modern high-field magnets and pulse techniques can be used to study the coordination environment of strontium cations in complex materials, a subject not yet explored with NMR. Further solid-state  $^{87}\text{Sr}$  NMR studies of additional strontium-saturated systems will provide added insight into the interactions of strontium cations with phyllosilicates, zeolites, and waste remediation materials.

**Acknowledgment.** This work was supported by the United States Department of Energy under Grant No. DE-FG07-99ER15012. G.M.B. also received support through a fellowship from the PSU Center for Environmental Chemistry and Geochem-

istry. S.K. acknowledges support by NSF Grant No. CTS-0242285 and the College of Agricultural Sciences under Station Research Project No. PEN03963. G.M.B. would like to thank Andrew S. Lipton (PNNL) for assistance with the experimental and computational methods used in this work. Part of the research described in this paper was performed in the Environmental Molecular Sciences Laboratory, a national scientific user facility sponsored by the Department of Energy's Office of Biological and Environmental Research and located at Pacific Northwest National Laboratory. Advanced computational facilities were provided with support from the PSU Center for Environmental Kinetics Analysis (NSF CHE-0431328). Support for the 11.74-T spectrometer at Penn State was provided by NSF Grant CHE-9601572.

## References and Notes

- (1) Vakulovsky, S. M.; Nikitin, A. I.; Chumichev, V. B.; Katrich, I. Y.; Voitsekhovich, O. A.; Medinets, V. I.; Pisarev, V. V.; Bovkum, L. A.; Khersonsky, E. S. *J. Environ. Radioact.* **1994**, *23*, 103.
- (2) Marceau, T. E.; Harvey, D. W.; Stapp, D. C.; Cannon, S. D.; Conway, C. A.; Deford, D. H.; Freer, B. J.; Gerber, M. S.; Keating, J. K.; Noonan, C. F.; Weisskopf, G. *History of the Plutonium Production Facilities at the Hanford Site Historic District, 1943–1990*; Hanford Cultural and Historic Resources Program, United States Department of Energy, 2002.
- (3) McKinley, J. P.; Zeissler, C. J.; Zachara, J. M.; Serne, R. J.; Lindstrom, R. M.; Schaef, H. T.; Orr, R. D. *Environ. Sci. Technol.* **2001**, *35*, 3433.
- (4) Zachara, J. M.; Smith, S. C.; Liu, C. X.; McKinley, J. P.; Serne, R. J.; Gassman, P. L. *Geochim. Cosmochim. Acta* **2002**, *66*, 193.
- (5) Chorover, J.; Choi, S. K.; Amistadi, M. K.; Karthikeyan, K. G.; Crosson, G.; Mueller, K. T. *Environ. Sci. Technol.* **2003**, *37*, 2200.
- (6) Dahl, S. G.; Allain, P.; Marie, P. J.; Mauras, Y.; Boivin, G.; Ammann, P.; Tsouderos, Y.; Delmas, P. D.; Christiansen, C. *Bone (New York, NY)* **2001**, *28*, 446.
- (7) Baud, C. A.; Very, J. M. *Colloq. Int. C.N.R.S.* **1975**, *230*, 405.
- (8) Das, R.; Nanda, B.; Patel, P. N. *J. Indian Chem. Soc.* **1983**, *60*, 693.
- (9) Komarneni, S.; Pidugu, R.; Amonette, J. E. *J. Mater. Chem.* **1998**, *8*, 205.
- (10) Komarneni, S.; Kozai, N.; Paulus, W. J. *Nature* **2001**, *410*, 771.
- (11) Komarneni, S.; Kodama, T.; Paulus, W. J.; Carlson, C. *J. Mater. Res.* **2000**, *15*, 1254.
- (12) Frazer, L. *Environ. Health Perspect.* **2002**, *110*, A528.
- (13) Chen, C. C.; Hayes, K. F.; Papelis, C. *Book of Abstracts*, 214th ACS National Meeting, Las Vegas, NV, September 7–11, 1997; American Chemical Society: Washington, DC, 1997; GE0C.
- (14) Chen, C.-C.; Papelis, C.; Hayes, K. F. *Adsorp. Met. Geomedia* **1998**, 333.
- (15) Chen, C.-C.; Hayes, K. F. *Geochim. Cosmochim. Acta* **1999**, *63*, 3205.
- (16) Sahai, N.; Carroll, S. A.; Roberts, S.; O'Day, P. A. *J. Colloid Interface Sci.* **2000**, *222*, 198.
- (17) O'Day, P. A.; Newville, M.; Neuhoff, P. S.; Sahai, N.; Carroll, S. A. *J. Colloid Interface Sci.* **2000**, *222*, 184.
- (18) Van Eck, E. R. H.; Janssen, R.; Maas, W. E. J. R.; Veeman, W. S. *Chem. Phys. Lett.* **1990**, *174*, 428.
- (19) Grey, C. P.; Veeman, W. S. *Chem. Phys. Lett.* **1992**, *192*, 379.
- (20) Grey, C. P.; Vega, A. J. *J. Am. Chem. Soc.* **1995**, *117*, 8232.
- (21) Gervais, C.; Veautier, D.; Smith, M. E.; Babonneau, F.; Belleville, P.; Sanchez, C. *Solid State Nucl. Magn. Reson.* **2004**, *26*, 147.
- (22) Larsen, F. H.; Skibsted, J.; Jakobsen, H. J.; Nielsen, N. C. *J. Am. Chem. Soc.* **2000**, *122*, 7080.
- (23) Bowers, G. M.; Lipton, A. S.; Mueller, K. T. *Solid State Nucl. Magn. Reson.* **2006**, *29*, 95.
- (24) Bastow, T. J. *Chem. Phys. Lett.* **2002**, *354*, 156.
- (25) Bowers, G. M.; Mueller, K. T. *Phys. Rev. B: Solid State* **2005**, *71*, 224112.
- (26) Weber, M. J.; Allen, R. R. *J. Chem. Phys.* **1962**, *38*, 726.
- (27) Garroway, A. N. *J. Magn. Reson.* **1977**, *28*, 365.
- (28) Cheng, J. T.; Ellis, P. D. *J. Phys. Chem.* **1989**, *93*, 2549.
- (29) Iuga, D.; Schafer, H.; Verhagen, R.; Kentgens, A. P. M. *J. Magn. Reson.* **2000**, *147*, 192.
- (30) Larsen, F. H.; Lipton, A. S.; Jakobsen, H. J.; Nielsen, N. C.; Ellis, P. D. *J. Am. Chem. Soc.* **1999**, *121*, 3783.
- (31) Schurko, R. W.; Hung, I.; Widdifield, C. M. *Chem. Phys. Lett.* **2003**, *379*, 1.
- (32) Lipton, A. S.; Sears, J. A.; Ellis, P. D. *J. Magn. Reson.* **2001**, *151*, 48.
- (33) Siegel, R.; Nakashima, T. T.; Wasylishen, R. E. *Chem. Phys. Lett.* **2004**, *388*, 441.
- (34) Bryce, D. L.; Gee, M.; Wasylishen, R. E. *J. Phys. Chem. A* **2001**, *105*, 10413.
- (35) Kentgens, A. P. M.; Iuga, D.; Kalwei, M.; Koller, H. *J. Am. Chem. Soc.* **2001**, *123*, 2925.
- (36) Smith, M. E. *Solid State Investigations of Less-Common Nuclei with Small Magnetic Moments*. In *Encyclopedia of Nuclear Magnetic Resonance*; Grant, D. M., Harris, R. K., Eds.; John Wiley: Chichester, New York, 1996; p 607.
- (37) Paulus, W. J.; Komarneni, S.; Roy, R. *Nature* **1992**, *357*, 571.
- (38) Lipton, A. S.; Heck, R. W.; Sears, J. A.; Ellis, P. D. *J. Magn. Reson.* **2004**, *168*, 66.
- (39) Bak, M.; Rasmussen, J. T.; Nielsen, N. C. *J. Magn. Reson.* **2000**, *147*, 296.
- (40) Park, M.; Lee, D. H.; Choi, C. L.; Kim, S. S.; Kim, K. S.; Choi, J. *Chem. Mater.* **2002**, *14*, 2582.
- (41) Bronnimann, C. E.; Zeigler, R. C.; Maciel, G. E. *J. Am. Chem. Soc.* **1988**, *110*, 2023.